Waste Management 161 (2023) 142–155

Contents lists available at ScienceDirect

Waste Management

journal homepage: www.elsevier.com/locate/wasman

Comparing the quantity and quality of glass, metals, and minerals present in waste incineration bottom ashes from a fluidized bed and a grate incinerator

Dominik Blasenbauer [a,b,*], Florian Huber [b], Julia Mühl [a], Johann Fellner [b], Jakob Lederer [a,b]

[a] Christian Doppler Laboratory for a Recycling-based Circular Economy, Institute of Chemical, Environmental and Bioscience Engineering (ICEBE), TU Wien, Getreidemarkt 9/166, 1060 Vienna, Austria
[b] Christian Doppler Laboratory for Anthropogenic Resources, Institute for Water Quality and Resource Management, TU Wien, Karlsplatz 13/226, 1040 Vienna, Austria

ARTICLE INFO

Keywords:
Municipal solid waste incineration
Bottom ash
Grate furnace
Fluidized bed combustion
Recycling
Circular economy

ABSTRACT

Bottom ash is the primary solid residue arising from municipal solid waste incineration. It consists of valuable materials such as minerals, metals and glass. Recovering these materials from bottom ash becomes evident when integrating Waste-to-Energy within the circular economy strategy. To assess the recycling potential from bottom ash, detailed knowledge of its characteristics and composition is required. The study at hand aims to compare the quantity and quality of recyclable materials present in bottom ash from a fluidized bed combustion plant and a grate incinerator, both located in the same city in Austria and receiving mainly municipal solid waste. The investigated properties of the bottom ash are grain-size distribution, contents of recyclable metals, glass, and minerals in different grain size fractions, and the total and leaching contents of substances in minerals.

The study results reveal that most recyclables present are of better quality for the bottom ash arising at the fluidized bed combustion plant. Metals are less corroded, glass contains fewer impurities, minerals contain fewer heavy metals, and their leaching behavior is also favorable. Furthermore, recoverable materials, such as metals and glass are more isolated and not incorporated into agglomerates as observed in grate incineration bottom ash. Based on the input to the incinerators more aluminum and significantly more glass can potentially be recovered from bottom ash from fluidized bed combustion. On the downside, fluidized bed combustion produces about five times more fly ash per unit of waste incinerated, which is currently disposed of in landfills.

1. Introduction

In many countries, including most EU member states, incineration is an essential municipal solid waste (MSW) treatment technology (Pomberger et al., 2017; Scarlat et al., 2019). The main solid residues from MSW incineration are incinerator fly ash (IFA) and incinerator bottom ash (IBA). IBA is the material not carried along with the flue gas and discharged in the lower part of the combustion chamber. Depending on the firing technology (grate furnace, fluidized bed combustion, rotary kiln), 1–10 wt% of the incinerator input is transferred to IFA, and about 15–25 wt% ends up as IBA (Purgar et al., 2016). The annual IBA generation in the EU is about 19 million tonnes (Bruno et al., 2021). IBA consists of minerals (80–85 wt%) and metals (8–15 wt%) that can serve as secondary raw materials for producing construction materials or in metal recycling (Chandler et al., 1997; Chimenos et al., 1999; Holm and Simon, 2017; Huber et al., 2020). However, these secondary raw materials should not contain significant amounts of substances detrimental to the environment. Therefore, it is required to determine the properties of IBA for the assessment of the potential contribution of IBA-recycling to a circular economy (Van Caneghem et al., 2019). Consequently, many studies aimed to determine these IBA-attributes, (e.g. Alam et al., 2019; Chimenos et al., 1999; del Valle-Zermeño et al., 2017; Dugenest et al., 1999; Huber et al., 2019, 2020; Huber et al., 2021; Loginova et al., 2019; Morf et al., 2013; Muchova et al., 2009; Seniunaite and Vasarevicius, 2017; Vateva and Laner, 2020; Wei et al., 2011), which are summarised and analyzed in different review articles (Abdullah et al., 2019; Astrup et al., 2016; Blasenbauer et al., 2020; Dou et al., 2017; Luo et al., 2019; Šyc et al., 2020; Verbinnen et al., 2017). These works mainly address IBA from MSW-fed grate incinerators (GI), but less from MSW-fed fluidized bed combustors (FBC). This is not surprising since the vast majority of MSW is processed in GI and less in FBC (Fellner et al., 2015;

* Corresponding author.
E-mail address: dominik.blasenbauer@tuwien.ac.at (D. Blasenbauer).

https://doi.org/10.1016/j.wasman.2023.02.021
Received 3 October 2022; Received in revised form 29 January 2023; Accepted 18 February 2023
Available online 4 March 2023

List of abbreviations

Chemical elements

Al	Aluminum
As	Arsenic
Ca	Calcium
Cd	Cadmium
Cl	Chlorine
Co	Cobalt
Cr	Chromium
Cu	Copper
Fe	Iron
Hg	Mercury
K	Potassium
Mo	Molybdenum
Na	Sodium
Ni	Nickel
Pb	Lead
S	Sulfur
Sb	Antimony
Si	Silicon
Tl	Thallium

Acronyms

BADM	bottom ash dry matter
DM	dry matter
EU	European Union
FBC	fluidized bed combustion
GI	grate incinerator
IBA	incinerator bottom ash
IC	ion chromatography
IFA	incinerator fly ash
ICP-OES	inductively coupled plasma optical emission spectrometry
L/S	liquid to solid ratio
MBADM	mineral bottom ash dry matter
MFA	material flow analysis
MSW	municipal solid waste
PSD	particle size distribution
PSF	particle size fraction
TDS	total dissolved solids
wt%	weight-percent

Leckner and Lind, 2020). However, in countries like Austria, Canada, China, Japan, Sweden or the USA, 10–30 % of MSW incineration is FBC (Jung et al., 2004; Leckner and Lind, 2020; Republic of Austria, 2017a).

A few studies aimed to address MSW-fired FBC and its residues: Abbas et al. (2001) determined the total elemental composition, the mineralogy, the leaching behavior of major and trace elements, and the content and behavior of chromium compounds of IBA from a mainly MSW-fed FBC in Sweden. Jung et al. (2004) determined the total content of particularly valuable metals from IBA and IFA from MSW-fed GI and FBC in Japan. While IBA and IFA from the GI were analyzed separately, IBA and IFA from the FBC were mixed before laboratory analysis. This did not allow a distinction of the element contents between both residue types. Saikia et al. (2008) determined the elemental and mineral composition of IBA from waste-fed FBC in Belgium. However, it is not entirely clear whether the high calorific fraction, that is co-incinerated, derives from MSW or any other waste stream. Santos et al. (2013) continued the work of Saikia et al. (2008) by comparing the leaching behavior of aged IBA from MSW-fed GI, and MSW- and industrial-waste-fed FBC. The difference in feedstock influenced the total element contents and leaching behavior of the IBA produced. Abbà et al. (2014) determined the elemental composition and suitability as recycled aggregate in concrete of IBA from MSW-fed FBC in Spain. Another Spanish study by Maldonado-Alameda et al. (2023) investigated the suitability of FBC-IBA as the precursor of alkali-activated binders compared to GI-IBA. They assessed different IBA properties such as particle-size-distribution, the elemental composition of matrix elements, leaching behavior and the composition of crystalline and mineral phases in both IBA types.

Although these studies provide some valuable information on GI- and FBC-IBA, they do not provide a complete picture of essential attributes of IBA relevant from a circular economy and environmental sustainability perspective. As Brunner and Mönch (1988) and Riber et al. (2008) point out, general material flows of MSW incinerators are required for further investigations. Furthermore, the particle-size distribution (PSD) and the potential secondary raw material content in different particle-size fractions (PSF) are essential for IBA treatment and material recovery facilities (Šyc et al., 2020). Knowledge of the total and leaching contents of environmental- and product-quality impairing substances in the mineral fraction of IBA is relevant if this fraction should be used as construction material (Blasenbauer et al., 2020; Dou et al., 2017). This article aims to fill these gaps using IBAs generated at two MSW incineration plants designed as GI and FBC and compare them regarding the issues mentioned before. Specifically, the research questions in this article are: (1) What are the material flows of GI and FBC MSW incineration? (2) What is the particle-size distribution of IBA from GI and FBC? (3) Which particle sizes in GI and FBC IBA contain valuable materials (metals, glass, minerals)? (4) What is the recovery potential of recyclables from GI and FBC? (5) What is the total and leaching content of relevant substances in the mineral fraction of IBA?

2. Materials and methods

2.1. MSW incineration plants considered

Both investigated incinerators, designed as GI (type: horizontal double-motion overthrust grate, wet bottom ash discharge) and FBC (type: stationary, rotating fluidized bed, “ROWITEC-technology”, dry bottom ash discharge), are located in the same city in Austria. The GI has a capacity of 250,000 t/a and was described in detail in Huber et al. (2020) and Boehmer et al. (2006, p. 66). The FBC has an annual capacity of 100,000 t/a and is described in detail in Kirnbauer and Kraft (2017) and Krobath and Thomé-Kozmiensky (2004). The feedstock of the two plants consists mainly (>90 %) of MSW from households, which makes those two plants ideal for comparison regarding their output fractions. Differences in the feedstock of the two plants are that the FBC incinerates mainly pretreated MSW, and small amounts of sewage sludge (5–10 wt% of the input). Pretreatment means mixed MSW is shredded and classified into particle sizes of <125 mm (42 wt%), 125–250 mm (45 wt%), and > 250 mm (12 wt%). Ferrous metals are removed from the PSF 125–250 mm (equals about 1 % of input). The entire fraction < 125 mm and about 60 % of the fraction 125–250 mm, are incinerated in the FBC, while the remaining outputs of the pretreatment process are incinerated in three other GI plants. As a result, after pretreatment about 70 wt% of the initial MSW is the input to the FBC, while the remaining 30 wt% is divided among the three GI plants.

2.2. Sample collection and preparation including particle-size distribution

Between November 2017 and November 2018, fresh IBA from four MSW incineration plants – including the GI and the FBC investigated in the present study – was sampled. The sampling procedure, described in detail in Huber et al. (2020) for the IBA of three GI, also applies to the

sampling procedure of IBA from the FBC and is summarized herein. The sample collection was distributed over a one-year sampling period, at different seasons and on different weekdays. Each sample was a truck-load of 20 t, freshly delivered (not aged) IBA from the incineration plant, from which 3 t increment samples were randomly collected for further processing (Figure S1 and S2, supplementary document). Further sample processing consisted of dry sieving into PSFs of <4 mm, 4–8 mm, 8–12 mm, 12–16 mm, 16–50 mm and >50 mm using a XAVA Recycling LS12X vibrating screen (Figure S4 left, supplementary document). Subsequently, these PSFs were wet sieved on a sieve stack with about 5–10 l water per kg IBA to investigate its impact on leaching properties and to determine the quantity of adhering smaller particles to larger ones (Figure S3, supplementary document). The sieve stack was assembled from 4 mm, 2 mm and 0.5 mm sieves. The wash suspension consisting of the <0.5 mm fraction, the dissolved solids and the wash water was filtered using a Büchner funnel. Total dissolved solids (TDS) were determined by drying the filtrate at 105 °C. Also, all other PSFs were dried at the same temperature and weighed. The cumulative PSD was determined according to the following equations, where P_n is the percentage of the mass m of particles that pass a sieve with the mesh width d (m_d), in relation to the total mass of all particles m_{total}.

$$P_n = \frac{\sum_{d=1}^{d=n} m_d}{m_{total}} \times [100\%] \quad (1)$$

The share of the PSFs above $PSF_{d_i-d_j}$ were calculated using Eq. (2), where m_{d_j} is the mass of particles that pass through the upper mesh width, m_{d_i} is the mass of particles that pass through the lower mesh width, and m_{total} is the total mass of all particles.

$$PSF_{d_i-d_j} = \frac{m_{d_j} - m_{d_i}}{m_{total}} \times [100\%] \quad (2)$$

The PSD is illustrated as a cumulative diagram, starting with the smallest to the largest PSF. The PSFs are also expressed as graphs, but non-cumulative, starting with the largest to the lowest PSF, from left to right.

2.3. Hand sorting analysis

Washed PSFs with a diameter >2 mm were hand-sorted based on their visual appearance and magnetic properties. The following general material fractions and subfractions (the latter in brackets) were distinguished: metals (magnetic ferrous metals, weakly-magnetic ferrous metals (e.g. stainless steel), aluminum, copper, brass, coins, silver, gold), pieces containing different metals like electric motors and transformers (copper, magnetic ferrous metals, aluminum), batteries (minerals, magnetic ferrous metals, brass), minerals (glass, mineral material), and unburnt organic matter. Mineral material of the PSFs > 16 mm, potentially containing enclosed metals, was crushed with a vibrating roller (JCB VMD 70) (Figure S4 right, supplementary document). The crushed PSFs still >16 mm were hand-sorted according to the abovementioned procedure. Crushed PSFs <16 mm and the original PSFs 0.5–16 mm were dried at 105 °C and subsequently milled with a disc mill (Essa LM201 Pulverizing Mill). The resulting fraction was classified into a fraction <0.5 mm, considered as mineral fraction, into a fraction of mixed materials 0.5–2 mm, which was not further hand-sorted, and a fraction >2 mm, which underwent hand-sorting. Results are only presented for the main fractions from a quantitative point of view. These are aluminum, magnetic ferrous metals, weakly-magnetic ferrous metals, copper, brass, glass, unburnt organic matter and mineral material. The hand-sorting procedure is described in more detail in Huber et al. (2020).

2.4. Chemical analysis of mineral fractions

The chemical composition of the mineral fractions in IBA is essential for its recycling in the construction industry, which is limited by legal requirements on the total and leaching contents of selected substances (Blasenbauer et al., 2020). In addition, several more substances, such as oxides of Ca, Si, Al and Fe are of relevance if recycling in cement production is planned (Huber et al., 2019). The chemical analysis was only performed on minerals, as metals and impurities should be removed before recycling as construction material (Šyc et al., 2020; Verbinnen et al., 2017). Since washing of IBA is increasingly practiced in countries like Austria and Germany, only washed minerals were considered (Holm and Simon, 2017; Huber, 2020). Glass was also analyzed separately as technologies to extract glass for recycling from IBA are available (Šyc et al., 2020). Where applicable, the total and leaching contents of selected substances were compared to legal requirements for using minerals in road-construction (Republic of Austria, 2017a) and cement-clinker production (Republic of Austria, 2017b).

2.4.1. Total contents of substances in washed mineral fractions

Determining the total content of selected substances of the washed mineral material, glass, and the TDS in different PSFs is described in detail in Huber et al. (2019). These materials were milled to a particle size <0.5 mm using an Essa LM201 Pulverizing Mill. Subsequently, a hand-held X-ray fluorescence (XRF) device (NITON XL3t Air, analyzation mode "TestAll-Geo") was used to determine the total content of matrix elements (Al, Ca, Cl, Fe, S, Si and K). The total content of the elements As, Cd, Co, Cr, Cu, Hg, Mo, Na, Ni, Pb, Sb and Tl was determined by digesting the material with a mixture of HNO_3, H_3PO_4, and HBF_4 in a microwave oven (MLS-MWS Laboratory Solutions), followed by the chemical analysis using a PerkinElmer Optima 8300 ICP-OES (inductively coupled plasma optical emission spectroscopy) equipped with a SC-2DX FAST autosampler. Values are displayed for each PSF individually and are compared to literature values. The *weigthed average*$_j$ is calculated using Eq. (3), in which j is the substance, *PSF* is the particle size fraction, i is the index of each PSF, with a maximum of $i = n$, and c_{ij} is the concentration of substance j in PSF i.

$$weigthed\ average_j = \frac{\sum_{i=1}^{i=n} PSF_i \times c_{ij}}{\sum_{i=1}^{i=n} PSF_i} \quad (3)$$

2.4.2. Leaching of substances in washed mineral fractions

To investigate whether washed minerals of IBA are suitable for utilization in road-construction, Austrian authorities require a leaching test according to standard EN12457-4 (EN, 2002), using a liquid-to-solid (L/S) ratio of 10 L water per kg dry bottom ash (Republic of Austria, 2017a). Limit values for the elements and substances As, Cr, Cu, Mo, Ni, Pb, Sb, chloride and sulfate and the physical parameter pH value are defined and were assessed. The required heavy metals were determined using ICP-OES (same device as described in Section 2.4.1); chloride and sulfate were measured with ion chromatography (IC) using a Dionex ICS 900 IC.

2.5. Uncertainty ranges

Uncertainty ranges refer to the standard deviation from three IBA samples per investigated plant.

3. Results and discussion

3.1. Material flow analysis of the two MSW incineration plants under investigation

The material flow analysis (MFA) (Fig. 1), based on data obtained by the plant operator by weighing every truck entering and leaving the plant, highlights the different distribution of solid outputs between the GI and FBC plants. The input to the GI and the FBC is similar, with 92 % of municipal solid waste as the primary input fraction. The MSW to the

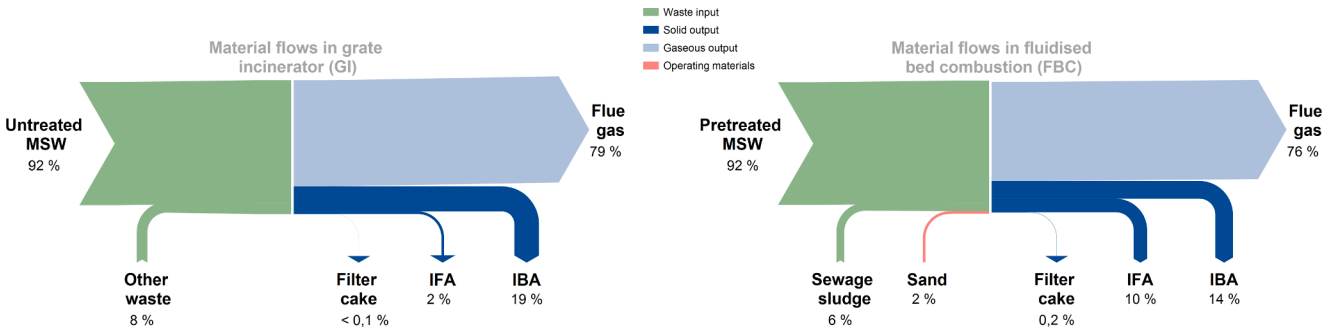

Fig. 1. Average material flows in weight-% for the GI plant (left) and the FBC plant (right). The data was obtained from the plant operator in 2021. Mean values of the years 2018–2020. Solid output flows are on dry basis. Incinerator fly ash (IFA); incinerator bottom ash (IBA); municipal solid waste (MSW). Note: the wastewater treatment facility, where filter cake is generated, receives wastewater from the FBC investigated in this work and other incinerators operating at the same industrial complex.

FBC is pretreated as outlined in Section 2.1. Additional waste inputs are 8 % other waste in the GI and 6 % sewage sludge in the FBC. A third input fraction to the FBC is 2 % sand to ensure a proper heat transfer in the fluidized bed.

The input-related total ash production (IBA + IFA) is 21 % and 24 % for the GI and FBC, respectively, and is therefore in a similar range. However, the ratio between IBA and IFA related to total ash production differs significantly. It is 90/10 for the GI and 58/42 for the FBC. Both values are in the range given by Leckner and Lind (2020). The significant differences between GI and FBC regarding IBA and IFA production are discussed in the following.

The FBC only incinerates pretreated waste with limited particle size (<250 mm) and sewage sludge. Moreover, parts of ferrous metals are removed before combustion. This, combined with more homogeneous but turbulent combustion conditions in a fluidized bed, leads to a better conversion of the input material causing more fine ash particles carried with the flue gas. Additionally, sand that forms the bed material in the FBC is partially transferred to the IFA through abrasion. As the amount of sand in the fluidized bed has to be constant, new sand is introduced to compensate for the abrasion losses. Regarding sand consumption, the literature suggests a relatively wide variation between 0.74 and 2.3 % of the FBC input (De Gisi et al., 2018; Leckner and Lind, 2020).

The GI, on the other hand, can process larger pieces of waste. In addition, the design of the furnace leads to a lower flue gas velocity. Both characteristics favor that particles remain on the grate and are not transferred into the flue gas, therefore not discharged as IFA.

3.2. Particle-size distribution

Fig. 2 shows the share of each considered PSF (left) and the cumulative PSD (right) of washed PSFs. GI-IBA has a much higher content of smaller particles than FBC-IBA. For instance, about 30 % of particles in the GI-IBA are ≤2 mm, and almost 60 % are ≤8 mm. In contrast, only 18 % of particles in the FBC-IBA are ≤2 mm, and 35 % are ≤8 mm. The PSF 0.5–2 mm is the largest fraction in the GI-IBA (19 %), whereas in the FBC-IBA, the largest fraction is 8–12 mm (24 %). The diameter D_{50}, which indicates that 50 % of the particles are smaller and 50 % are larger than this diameter, equals 6 mm for the GI-IBA and 10 mm for the FBC-IBA. In Šyc et al. (2018) and Caviglia et al. (2019), similar ranges for D_{50} (3–6 mm) for IBA from GI plants are given. In Maldonado-Alameda et al. (2023), the D_{50} value for GI-IBA is 4 mm, whereas the value for the FBC-IBA is slightly above 1 mm, which is different from the findings in the present work. Maldonado-Alameda et al. (2023) explain their high content of fine particles with the pretreatment before the incineration in the FBC. In a review by Dou et al. (2017), D_{50} ranges from 1 to 10 mm. However, it is not always entirely clear from which incineration type the IBA originated.

The low proportion of fine particles (especially <0.5 mm) in the FBC-IBA of this present work can be explained again by the specific design and operating conditions in an FBC plant. IBA is screened at 2 mm right after discharge to reduce sand consumption (Krobath and Thomé-Kozmiensky, 2004). All particles (sand and fine ash particles) smaller than this mesh size are fed back to the combustion chamber as bed material. Additionally, abrasion leads to a higher share of fine material, which tends to be carried along with flue gas and therefore does not remain in the IBA (see Section 3.1). From a recycling point of view, larger particle sizes are more desirable since it is easier to extract metals from these (Šyc et al., 2020). The concentrations of TDS are generally low, with values of 1.1 % for the GI-IBA and 0.15 % for the FBC-IBA.

3.3. Materials in different particle-size fractions

Fig. 3 shows the mass fractions of aluminum, magnetic ferrous metals, weakly-magnetic ferrous metals, brass, copper, glass, unburnt

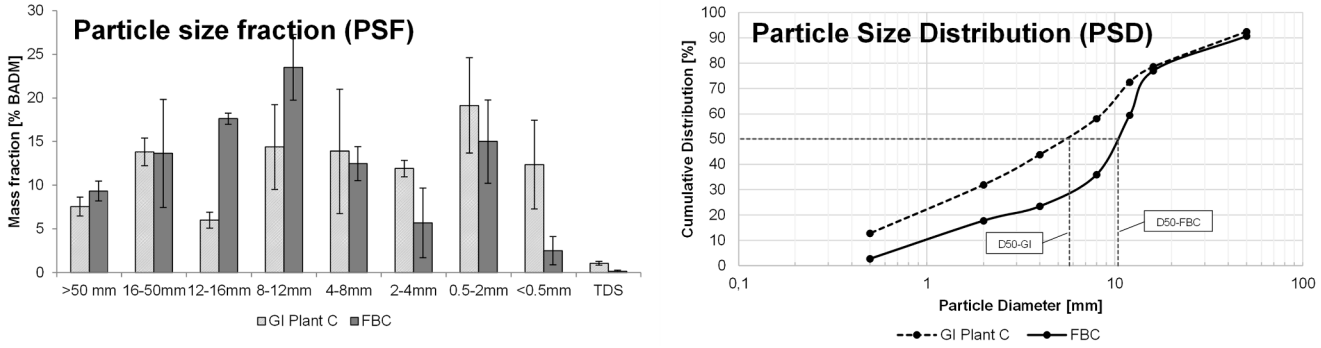

Fig. 2. Particle size fractions and cumulative particle size distribution of washed GI- and FBC-IBA related to total bottom ash dry matter (BADM). Total dissolved solids (TDS) are the fraction of bottom ash solubilized during the washing procedure. D_{50} − GI = 6 mm, D_{50} − FBC = 10 mm.

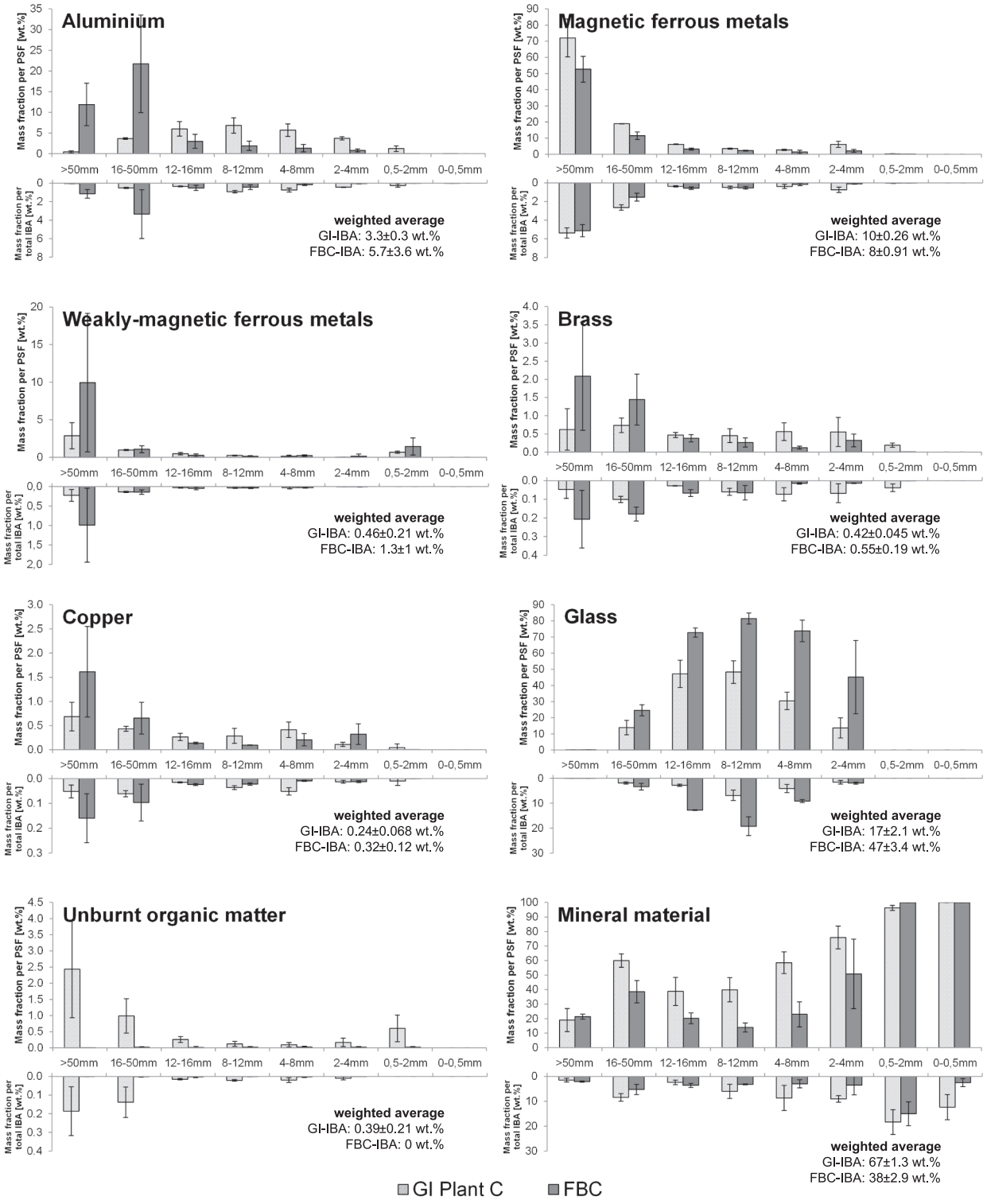

Fig. 3. Mass fractions of materials in washed GI- and FBC-IBA. Each material shown has (1) an upper graph showing the proportion of that material relative to the mass of that particle size fraction and (2) a lower graph showing the same material relative to the total IBA mass. Additionally, for each material, the weighted average content of this material is shown. All values refer to bottom ash dry matter.

organic matter and mineral material based on dry IBA matter. All materials, except for magnetic ferrous metals and mineral material, show higher concentrations in the FBC-IBA than in the GI-IBA. The most remarkable differences between the two incinerators can be seen in glass and weakly-magnetic ferrous metals. IBA from the FBC consists of 2.8 times more glass than the IBA from the GI. In addition to the high overall concentration, glass is with about 43 % also the largest single fraction in the FBC-IBA. The PSFs >8 mm contain about 70 % of the glass; more than 95 % of the glass can be found in the PSFs >4 mm. So far, attempts to recover glass from IBA as reported in literature have failed (Šyc et al., 2020). However, all those attempts were carried out with IBA from grate incinerators. Due to the lower, more homogeneous temperature

distribution in an FBC, which is in the range of 600–900 °C in general (Kolbitsch et al., 2012), and about 630 °C in the investigated FBC specifically (Kirnbauer and Kraft, 2017), glass is less likely to melt and form agglomerates with other materials such as metals and mineral phases, as shown in Fig. 4. In addition, the dry discharge of the IBA in an FBC favors cleaner fractions, which are less contaminated with extraneous materials (less caking) that lower the quality and make the recovery of glass more complex (see Fig. 4, top row). The weakly-magnetic ferrous metals content, that is 2.8 times higher in the FBC-IBA compared to the GI-IBA, can be traced back to one sample, which contained about five times more weakly-magnetic ferrous metals than the other samples. This indicates a high variability of the content of this metal. Regarding aluminum, contents are by a factor of 1.7 higher in the FBC- than in GI-IBA. In that case, lower bed temperatures in the FBC (Leckner and Lind, 2020) may reduce oxidation processes, preserving aluminum in its metallic form (Hu et al., 2011). This is supported by the fact that the non-metallic aluminum concentration in the GI-IBA mineral fraction is significantly higher than in the FBC-IBA (cf. Fig. 5). How significant the

Fig. 4. Glass (1st row), aluminum (2nd row), and magnetic ferrous metals (3rd row) fractions of IBA from GI (left) and FBC (right). 4th row: Mineral fractions of IBA from GI (left) and FBC (middle). Agglomerate of glass, metals and mineral phases in GI-IBA (right).

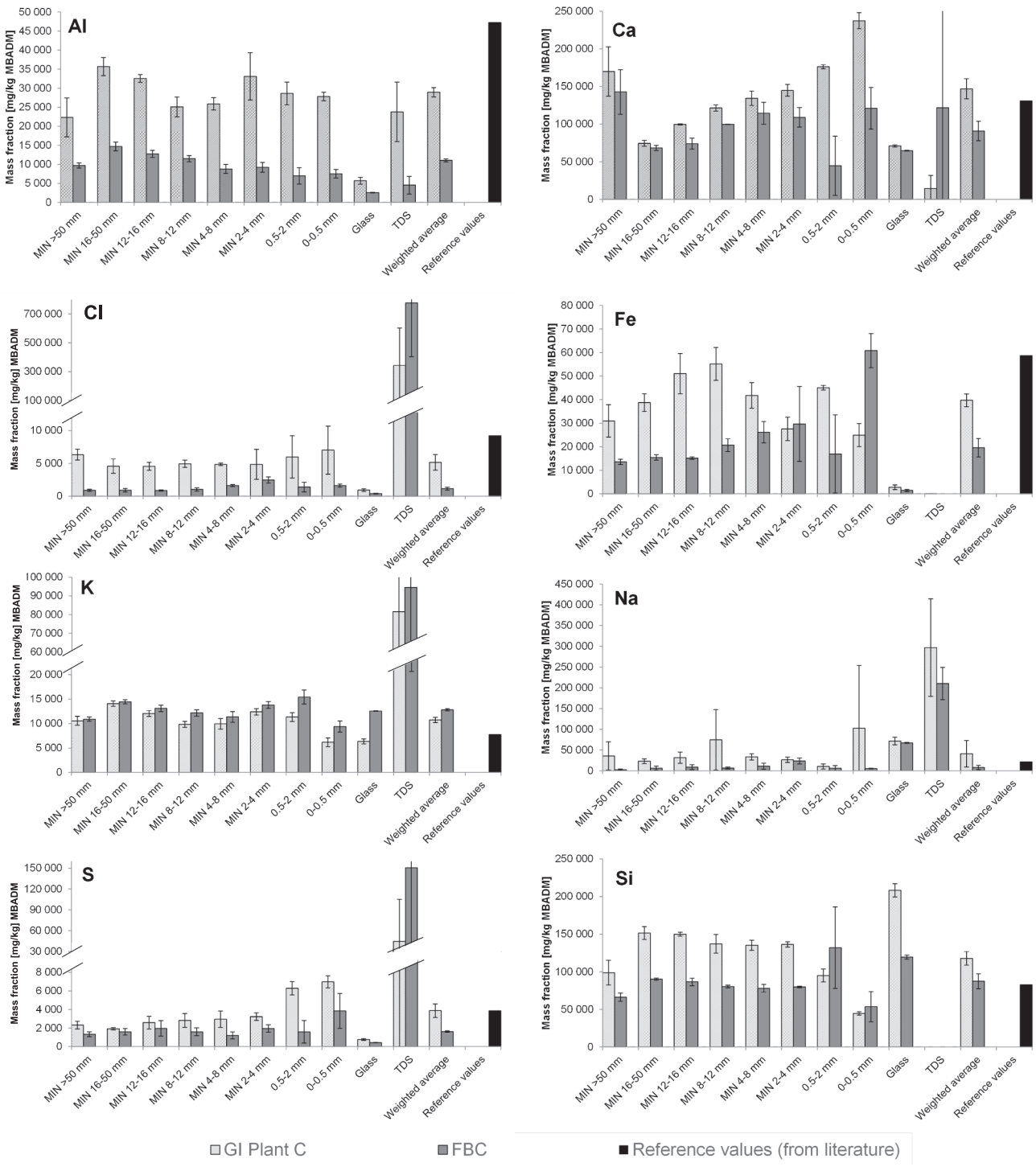

Fig. 5. Matrix elements in the different PSF of minerals (MIN), glass, and total dissolved solids fraction of IBA from GI and FBC in mg/kg mineral bottom ash dry matter (MBADM). Reference values refer to literature data for bottom ashes provided by Hjelmar et al. (2013). Note: Only in PSFs >2 mm it was possible to distinguish between minerals and non-mineral materials. Therefore, below 2 mm the entire fraction (mineral and non-mineral material) was used in the analysis.

effect of oxidation is, is still a subject of debate and needs to be further investigated (Šyc et al., 2020). Brass and copper contents are by a factor of 1.3 higher in the FBC-IBA, which is possibly caused by variations in the incinerators' waste input. Magnetic ferrous metals are also by a factor of 1.3 higher in GI-IBA, while minerals are higher by 1.8. The lower content of ferrous metals in the FBC-IBA can be explained by the pretreatment of the input material, where parts of the ferrous metals are removed from the input fraction 125–250 mm prior to incineration. In the FBC-IBA, most materials are concentrated in fractions >4 mm. Only mineral materials are also found in the smaller PSFs. Finally, the average content of unburnt matter in the GI-IBA is as low as 0.39 %. Only some isolated pieces of unburnt matter were found in the FBC-IBA, which means that the total content of this material can be considered to be zero.

In Fig. 3 each diagram also includes a lower graph showing the same material relative to the total IBA mass. This is important since the

concentration of a certain material in a particular PSF might be very high, but if this PSF is only of minor importance, the overall concentration of this material can be much lower. Example: The magnetic ferrous metals content in the GI-IBA in the PSF >50 mm is as high as 70 % (Fig. 3, magnetic ferrous metals, top graph). However, the PSF > 50 mm is only about 7 % of the total mass. As a result, the magnetic ferrous metals larger than 50 mm are only about 5 % overall (Fig. 3, magnetic ferrous metals, lower graph).

Regarding metal recycling, PSFs larger than 12 mm are the most interesting fractions in the FBC-IBA. 82 % of the total brass content is in this PSF, 88 % of the copper, 88 % of the aluminum, 91 % of the magnetic ferrous metals and 94 % of the total weakly-magnetic ferrous metals content. In comparison, the same PSF of the GI-IBA also contains the majority of the magnetic- and weakly-magnetic ferrous metals (about 84 % of their total content). However, only 27 % of aluminum, 43 % brass, and 54 % copper are in this PSF. To achieve similar recovery potentials for aluminum and brass, they must be recovered from the PSFs >2 mm, and for copper from the PSFs >4 mm. A reason for the concentration of these metals in the smaller particle-sizes of the GI-IBA could be the heterogeneous temperature distribution on the grate. Temperatures of over 1000 °C can be reached on a grate (Vandecasteele et al., 2007) and even up to 1400 °C on the surface of waste particles (Wissing et al., 2017). At these temperatures, metals like aluminum, brass and copper melt (partially mineralize due to nitrification or corrosion) and concentrate finely dispersed in droplets in smaller particle sizes. Hu et al. (2011) investigated this phenomenon for aluminum at temperatures above 810 °C, a temperature which is in the range of FBC but not of GI. They found that previously lumpy and flat aluminum pieces form droplets – especially if salts are present, which can facilitate the coalescence of aluminum droplets. Similar observations were obtained by Bunge (2018), who found that above 660 °C molten aluminum trickles through the firebed and solidifies at the colder grate surface.

Higher contents of valuable metals and a significantly higher glass content in the FBC-IBA are mainly facilitated by the input to the furnace, operating conditions, and design. As shown in Fig. 1, considerably more of the input to the FBC is transferred to the IFA, increasing the relative content of metals and glass in the IBA. To consider this, the recovery potentials of valuable materials are compared between the two incinerators in the subsequent section.

3.4. Recovery potential of recyclables from GI and FBC

As previously discussed, both incinerators produce significantly different amounts of IBA, which impedes a direct comparison of the recovery potential of recyclables from the two technologies. Despite this fact, this section assesses the recovery potential of aluminum, magnetic ferrous metals, weakly-magnetic ferrous metals, brass, copper and glass from IBA, based on the input to the respective incinerator. This method considers the different IBA generation rates and directly compares the two incineration technologies regarding recycling material recovery.

A review by Šyc et al. (2020) showed that advanced treatment technologies for IBA could recover metals from particle sizes starting at 2 mm (in specific cases even below). Therefore, 2 mm is the cut-off particle size considered for the calculation. Table 1 depicts the results of this assessment, where the recovery potentials are shown in *kg per 1000 kg of waste input* to the respective incinerator.

Table 1
Recovery and recycling potential in PSFs larger than 2 mm per 1000 kg of waste input to the two different incinerators.

	GI	FBC
	kg/1000 kg waste input	
Aluminum	5.6	7.5
Magnetic ferrous metals	19	11
Weakly-magnetic ferrous metals	0.85	1.7
Brass	0.70	0.73
Copper	0.43	0.43
Glass	32	62

Considering the high standard deviation of brass and copper in the FBC-IBA, which may indicate a high fluctuation in the content of these materials, it can be assumed that equally high recovery potentials for brass and copper are in both IBAs. More significant are the differences for aluminum, where higher amounts can potentially be recovered from the FBC-IBA. Beside a different composition of the input, the most obvious explanation are lower oxidation rates in the FBC due to lower temperatures (see Section 3.3). Only about half as much magnetic ferrous metals can be found in the FBC-IBA, resulting from the pretreated waste input to the FBC (see Section 2.1). As previously discussed, the PSF >50 mm of one FBC-IBA sample contained five times more weakly-magnetic ferrous metals than the other samples, which is also reflected in this calculation. If this outlier would be excluded from the calculation, then the difference between GI and FBC would be much smaller. The most remarkable difference is for glass, where per 1000 kg waste input almost twice as much can be recovered from the FBC if compared to the GI. This large difference can hardly be explained by variations in the input.

The discussed similarities and the differences allow two conclusions: (1) Similar recovery potentials for copper, brass and weakly-magnetic ferrous metals suggest that the input to both incinerators is relatively similar. It can be assumed that these materials are less affected by the harsh environment in an incinerator than other materials and are therefore transferred through the plant almost unchanged. The same may apply for magnetic ferrous metals if not removed during the pretreatment. (2) The differences show that for some materials, such as aluminum and glass, the type of incineration technology can affect the recoverability of those materials. Lower, more homogeneous temperatures generate fewer melt products, lead to less oxidation in combination with a dry discharge of IBA and leave particles almost unchanged in size. The latter is especially important for aluminum since the most widely used eddy current separators can separate particles with a size >5 mm (Šyc et al., 2020). Most of the aluminum in FBC-IBA is present in the PSFs >16 mm.

3.5. Chemical composition of mineral IBA fractions

3.5.1. Total contents of matrix substances

Fig. 5 shows the total content of matrix substances in the washed mineral fractions of IBA from GI and FBC per PSF and the weighted average. In the quantitatively most relevant mineral fractions, Al, Fe and Si concentrations show significantly higher values in the GI-IBA compared to the FBC-IBA. Other substances such as Ca, Na and K are in a similar range for both IBAs.

Matrix elements such as Ca, Cl, Na, S, Si and K of the GI-IBA are in good agreement with literature values provided by Hjelmar et al. (2013), which are also shown in Fig. 5. For Al and Fe, literature values are clearly higher than the measured values of the investigated GI-IBA. Values for Al, Fe and S also tend to be higher in the study by Loginova et al. (2019). In the present work, only mineral IBA-components were analyzed. Higher Al and Fe concentrations could result from different sample preparation and pretreatment of IBA. Because Hjelmar et al. (2013) processed and statistically evaluated data from numerous ash samples from GIs in different European countries, it is unknown how the sample preparation was carried out and which constituents were considered. Furthermore, it is unknown whether washed or unwashed samples were used for the analysis. In Loginova et al. (2019), the concentrations of Ca, Na and Si correspond well with measured contents in GI-IBA of the present study. No clear correlation between increase or decrease and particle-size can be found. Regarding matrix elements in the FBC-IBA, the content of Ca, K and Si are comparable to literature values; other such elements show lower concentrations in the FBC-IBA.

As shown in Section 3.2, TDS play, due to their overall low

concentrations, only a minor role in both IBAs. Still, remarkably high concentrations of Ca, Cl and S in the TDS of the FBC-IBA can be observed – presumably due to the dry IBA discharge. In a wet discharging system – like installed in most GIs – soluble components are dissolved and separated from the IBA.

3.5.2. Total contents of trace elements

In Fig. 6, trace element contents in the two IBAs are compared with the limit values (horizontal lines) according to Austrian regulations for recycling mineral materials from IBA in road-construction and cement-clinker production (Republic of Austria, 2017a, b). For reference, values are compared to literature data provided by Hjelmar et al. (2013) again.

The trace element concentrations in the GI-IBA tend to be higher than in the FBC-IBA. The most considerable differences can be observed for the elements Sb (15 vs 0.41 mg/kg) and Tl (7.2 vs 0.29 mg/kg). The very low standard deviation indicates little variation between samples of each IBA. Reasons for these significant differences could be that less of these two elements are generally supplied in the FBC; however, since the input to the plants is similar, this is unlikely. Another reason may be an increased transfer to the IFA, so that they cannot be found in the IBA. Both, del Valle-Zermeño et al. (2017) and Loginova et al. (2019), have shown that Sb tends to be enriched in finer fractions. As shown in Fig. 2, the fine fraction (<0.5 mm) in the FBC ash is much smaller than in the GI, suggesting a transition into the IFA. Furthermore, these significant differences may be due to the higher tendency of these elements to transfer into the washing water during wet screening. This is indicated by the much higher contents of these two elements in the TDS of the FBC-IBA compared to the GI-IBA.

Slightly higher concentrations of trace elements in the FBC-IBA can only be found for the elements As and Hg. Generally, measured concentrations in both investigated IBAs are in a similar range compared to the literature (Hjelmar et al., 2013). Remarkably high literature values were found for the elements Hg and Sb. The concentrations of Cr and Pb correspond well to the values obtained by Loginova et al. (2019), while Ni and Sb concentrations are slightly lower.

For utilization in road-construction, the elements Cd, Cr, Ni and Pb have to be considered (Republic of Austria, 2017a). The weighted average contents of Cd and Cr in the GI-IBA exceed the limit values, which can be traced to the PSF 0.5–2 mm. Values for Pb are slightly below the limit, whereas values for Ni are well below the limits. Contrary to GI-IBA, the weighted average contents of all required elements in FBC-IBA pass the threshold for utilization in road-construction. Only individual PSFs would exceed the limit values for Cd (PSFs 12–16 mm, 8–12 mm and 0.5–2 mm), Cr (PSFs 4–8 mm and 2–4 mm), Ni (PSF 0–0.5 mm), and Pb (PSF 2–4 mm).

To use IBA in cement clinker production, the total contents of As, Cd, Co, Cr, Hg, Ni, Sb and Tl have to comply with limit values defined by the Republic of Austria (2017b). The weighted average contents of Cd and Cr of both IBAs are above the limit value. Additionally, Pb and Tl contents in the GI-IBA exceed the limit values. This is also the case for the As content in FBC-IBA. These elevated values are marginal for FBC-IBA, whereas Cd, Cr, and Pb contents in the GI-IBA are more significantly above the limit values. In most cases, small PSFs are responsible for exceeding the limit values. However, utilization in cement-clinker production would still be possible if the substitution of raw meal is limited to 10 %, and the produced cement complies with the requirements in the corresponding guideline (Republic of Austria, 2017b).

Certain heavy metals (e.g. Cd, Cr, Pb) tend to be increased in particle sizes <2 mm, which in the case of GI-IBA accounts for more than one-third of the total PSD (see Fig. 2). Huber et al. (2019) found similar results in IBA originating from two other grate incinerators in Austria. Caviglia et al. (2019) found this effect for Pb, Ni and Ti, while Cr and Cu tend to concentrate in coarser PSFs. Regarding Cr, this observation does not correspond to the findings of this present investigation. del Valle-Zermeño et al. (2017) also investigated the correlation between particle size and heavy metal content. They found increased concentrations of Cd, Cu, Mn, Ni, Sb, Ti, Pb, Zn in particle sizes smaller than 2 mm. As, Cr, Mo and Sn also have their peak concentrations below 2 mm, but slightly increase again towards larger particles. Alam et al. (2019) suggest removing particles <0.125 mm since this fraction is found to be most enriched with heavy metals.

A possible improvement for the two investigated IBAs, would be removing the particles <2 mm after their discharge from the incinerator. This measure would reduce the total concentration of heavy metals, which, in turn, would benefit the utilization of the mineral fraction of IBA. In addition, removing particles smaller than 2 mm after discharging also results in improved metal recovery since binding reactions associated with the wet discharge of IBA are reduced (Bunge, 2018).

Glass can also be a carrier of trace elements. Compared to the FBC-IBA, the glass fraction in the GI-IBA contains some of these elements at significantly higher concentrations. Viczek et al. (2020) found that As, Cd, Cr, Ni, Pb and Sb can serve for instance as additives or pigments in glass production, which are potential carriers for such elements. Thus, glass extraction might help reduce the contents of trace elements (Mühl et al., 2022). However, not only can glass itself be a carrier for heavy metals but small extraneous non-glass materials adhering to glass particles. Loginova et al. (2019) and the literature therein identified such particles attached to larger particles resulting from the quenching of IBA and concluded that their structure facilitates the absorption (and release during leaching tests) of heavy metals to their surface. Fig. 4 depicts that glass in the GI-IBA is much more coated in small particles – even after wet-sieving – than glass in the FBC-IBA. This might explain why the total content of certain elements in the glass fraction in the GI-IBA is significantly above the content of the glass fraction in the FBC-IBA. Furthermore, if glass recovery from IBA is an option, sensor-based sorting of less coated materials is more efficient. The recovered glass should also be subjected to lead glass removal to reduce the lead content (see Fig. 6).

TDS do not carry significant amounts of the discussed trace elements – with three exemptions: Hg, Sb and Tl in the FBC-IBA. However, the high standard deviation indicates that the transfer of these elements to the washing solution during wet screening is highly variable. Only low concentrations of the other measured elements can be found in the TDS, showing that solely wet screening does not remove these substances efficiently.

3.5.3. Leaching contents of substances in the washed mineral fractions of IBA

Comparing the leaching behavior between the two investigated IBAs shows that GI-IBA consists of more soluble components than FBC-IBA, indicated by higher chloride content and electric conductivity (Fig. 7).

For utilization of IBA in road construction, leaching limit values for pH value, chloride, sulfate, As, Cr, Cu, Mo, Ni, Pb and Sb contents are defined (Republic of Austria, 2017a). Concentrations of Cr and Sb in the GI-IBA leachate are above the limit values and prevent utilization in road construction. One GI-IBA sample has significantly elevated Cr values in all PSFs and is therefore responsible for exceeding the limit. For Sb, consistently all IBA samples exceed the leaching limit in all grain size fractions. For FBC-IBA, Sb is also responsible for the fact that this IBA cannot be utilized in road construction. Possible reasons and causes for heavy metal leaching from IBA are discussed below.

In addition to the parameters relevant for utilization in road-construction, the leachate concentrations of the elements Cd, Co, Hg and Tl were measured. The concentrations of Cd, Co and Tl are below their respective limit of detection (LOD) of 0.018 mg/kg, 0.09 mg/kg and 0.16 mg/kg. Average concentrations of Hg in the GI-IBA are 0.01 mg/kg and 0.023 mg/kg in the FBC-IBA. The LOD for Hg is 0.003 mg/kg.

Since glass separation from IBA is not widely practiced, knowing its leaching behavior in wet environments is a valuable information. The pH value of the glass leachate from the GI-IBA is about one pH unit above the FBC-IBA. Moreover, significantly more chloride and Cr, and slightly more As are released from the glass of the GI-IBA. In contrast, glass from the FBC-IBA releases slightly more Mo and Ni to the leachate.

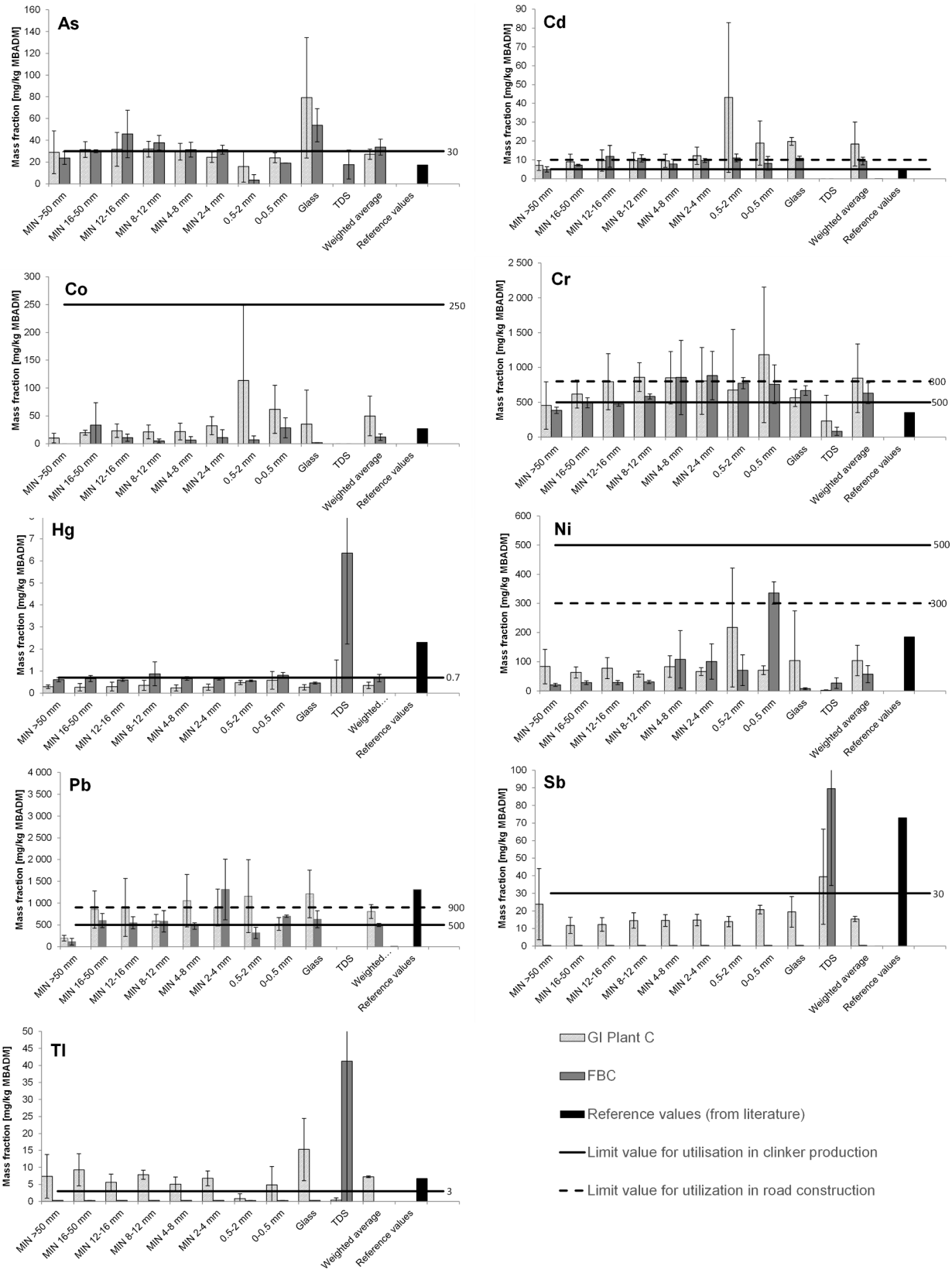

Fig. 6. Trace elements in the different PSF of minerals, glass, and total dissolved solids fraction (TDS) of IBA from GI and FBC in mg/kg mineral bottom ash dry matter (MBADM). Total dissolved solids are the fraction of bottom ash solubilized during the washing procedure. Reference values refer to literature data for bottom ashes provided by Hjelmar et al. (2013). Note: Only in PSFs >2 mm it was possible to distinguish between minerals and non-mineral materials. Therefore, below 2 mm the entire fraction (mineral and non-mineral material) was used in the analysis.

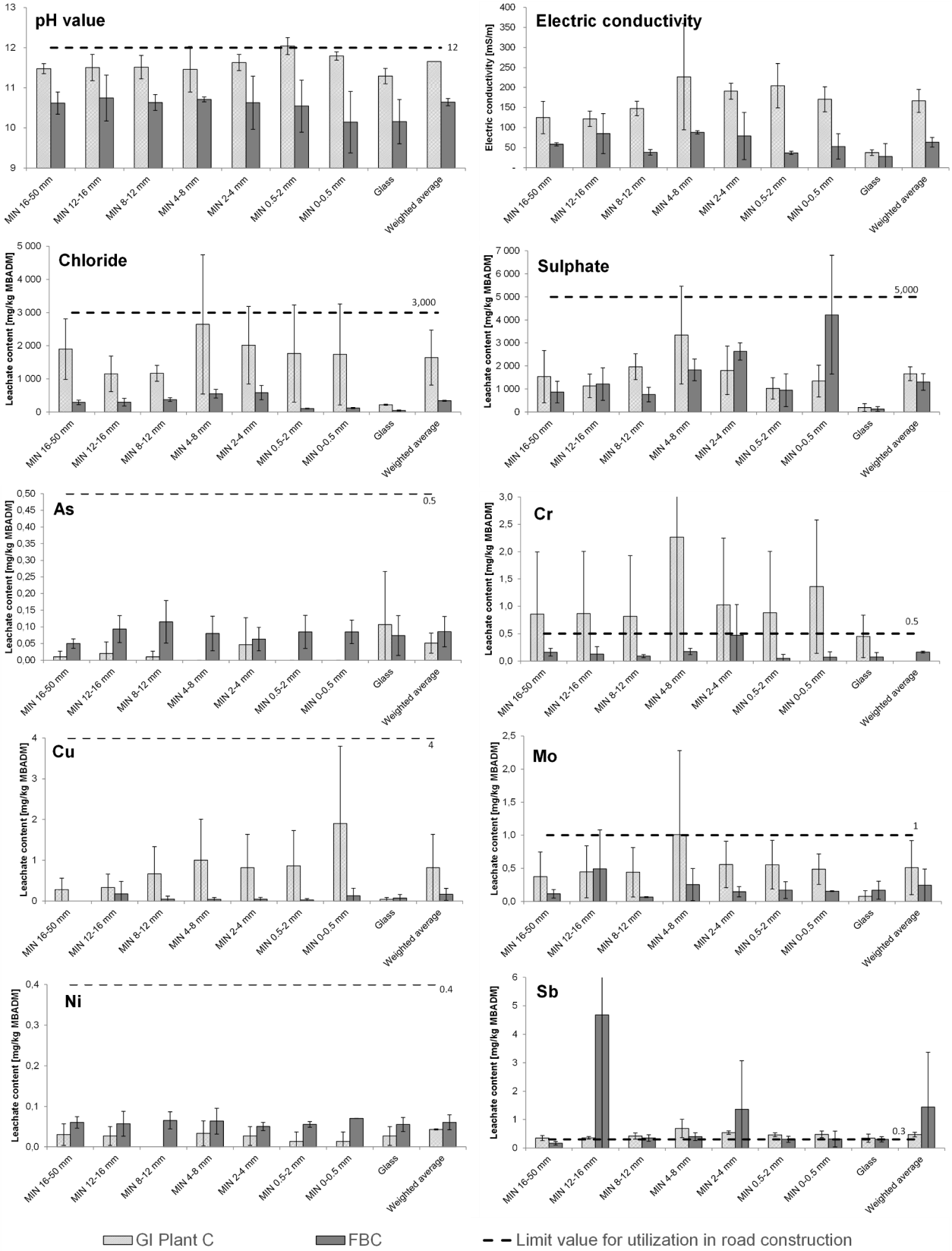

Fig. 7. Leaching behavior of substances in the different PSF of minerals and glass fraction of IBA from GI and FBC in mg/kg mineral bottom ash dry matter (MBADM). Although limit values for Pb are defined, measured values for Pb are not shown in the diagram because concentrations are below the detection limit (0.036 mg/kg) and therefore meet the limit value defined at 0.5 mg/kg. Note: Only in PSFs >2 mm was it possible to distinguish between minerals and non-mineral materials. Therefore, below 2 mm the entire fraction (mineral and non-mineral material) was used in the analysis.

Astrup et al. (2016) and the literature therein, point out that a particular leaching behaviour is less driven by the waste input to the incinerator, the operating conditions or the total content of a specific element (except highly soluble salts of Na, K and Cl) but by dissolution/precipitation reactions of mineral phases present in the IBA. Furthermore, specifically weathered IBA interacts with reactive surfaces and complexing components.

An explanation for elevated heavy metals leaching rates is the higher pH value of the GI-IBA-leachate compared to FBC-IBA-leachate. Verbinnen et al. (2017) show that the leaching behavior of certain heavy metals, such as Cu, strongly depends on the pH value. Low and high pH values facilitate the leaching of Cu, whereas at pH values around 9–10 leaching rates reach a minimum. In contrast, Sb reaches its leaching maximum at pH values around 8–9, whereas leaching rates decrease at lower and higher values. Chandler et al. (1997) published data from hundreds of IBA samples investigating the dependency between the pH value and the leaching rate of several heavy metals. For As, no clear correlation between the pH and the solubility was found. This present data also reflects that contents of As in the FBC-IBA-leachate are generally slightly above the ones from the GI-IBA, although the pH value of the FBC-IBA-leachate is lower. For glass this is exactly vice versa: the pH value of the GI-IBA-glass-leachate is high, As content therein is as well higher than in the FBC-IBA. For Cd, Cr, Cu and Mo, a wide range between pH value and solubility was found by Chandler et al. (1997); however, all of these elements tend to leach more at high pH values around 11–12. Our measurements also reflect this finding for Cr, Cu and Mo. Cd leaching values are for both investigated IBAs below the limit of detection. For Ni, Chandler et al. (1997) describe a decreasing solubility with an increasing pH value. This could be a another explanation for the consistently higher Ni contents in the leachate of the FBC-IBA. Pb concentrations in the leachate of both IBAs are below the limit of detection of 0.036 mg/kg. This finding is interesting since Pb leaching increases at pH values above 11 (Chandler et al., 1997), which is the case for the leachate of the GI-IBA (pH 11.6). In contrast, the pH value of the FBC-IBA leachate is 10.7.

Verbinnen et al. (2017) and Chandler et al. (1997) also point out that the presence of organic matter is detrimental to the leaching rates of Cu in particular, as well as Ni, Pb and Zn. Organic matter present as acids in combination with an alkaline environment in the leachate forms highly soluble complexes with cations of the previously mentioned heavy metals (Verbinnen et al., 2017). Although the unburnt matter content is relatively low in the GI-IBA, it is still significantly higher than in the FBC-IBA. This fact may be a possible explanation for tendencies toward higher leaching rates of heavy metals in GI-IBA.

Caviglia et al. (2019) found amorphous mineral phases, combined with heavy metals in these phases to be potentially responsible for higher leaching rates of heavy metals. Alam et al. (2019) found that up to one-third of the IBA's composition consists of amorphous phases containing significant amounts of heavy metals. Amorphous mineral phases are products of the quenching process of IBA in the wet discharging system of a typical GI incinerator. Since such a wet discharging system for IBA is installed in the GI under investigation, this could explain higher leaching rates for some heavy metals. This hypothesis is supported by the fact that only in the GI-IBA agglomerates composed of molten glass, metals and mineral phases were found (see Section 3.3).

Since significant Sb leaching prevents both IBAs from being utilized in road construction, it is discussed in more detail in this paragraph. Johnson et al. (1999) investigated the leachate composition of an IBA landfill in Switzerland and revealed that Sb leaching directly corresponds to the Ca concentration of IBA. Cornelis et al. (2006) and Cornelis et al. (2012) investigated this phenomenon more deeply. They found that carbonation of IBA and the resulting decrease of the pH value of the leachate below 12 leads to increasing leachability of Sb. More recently, Kalbe and Simon (2020) and Simon et al. (2021) carried out long-term lysimeter leaching tests where a decreasing Ca concentration due to carbonation clearly leads to an increasing Sb leaching rate. Both, Kalbe and Simon (2020) and Simon et al. (2021), conclude that wet treatment has, in general, positive effects on the leaching behavior of IBA; however, regarding Sb leachability, it is detrimental and a technically applicable solution for this issue is yet to be found.

These findings regarding Ca and Sb interaction can explain the high Sb leaching contents in the GI-IBA. In the supplementary file, Table S16, total and leachate content values measured are compared with the results from Kalbe and Simon (2020) (batch leaching test at L/S 10). It is shown that the total Ca content in our measurements is considerably higher, while the Sb content is only one-third. For the leachate contents, the situation is vice versa. In the present case, considerably less Ca was leached but almost three times more Sb compared to the measurements in Kalbe and Simon (2020).

However, this does not explain the two outliers in the size fractions 12–16 mm and 2–4 mm in the FBC-IBA. The measured values are also shown in Table S16. These measurements do not have exceptionally high standard deviations (see bold Sb values in Table S16). The total Ca and Sb contents and the pH of the leachate are almost the same for all three samples. The Ca content in the leachate varies and offers no consistent explanation for the high Sb values in the leachate. Very little Sb is present in this ash (0.41 mg/kg in FBC-IBA vs 15 mg/kg in GI-IBA). All these points are, therefore, not very likely to be the source of the outlier. A possible explanation could be that one or more individual particles contained an exceptionally high amount of Sb, which leached out during the leaching test. Since only minerals were used in this test (metal and glass were sorted out), a possible source could be ceramic shards with glazes containing a lot of Sb. Turner and Filella (2020), found ceramicware with Sb contents ranging from 308 to 62,800 mg/kg. In Fig. 4, ceramic shards can be seen in the FBC and the GI-IBA. It can be speculated whether these shards are rich in Sb and contribute to high Sb contents in both IBA-leachates.

4. Conclusion

GI-IBA and FBC-IBA contain substantial portions of recyclable materials (metals, minerals, glass). Recovering these recyclables from IBA can contribute to achieving recycling targets to comply with sustainable development initiatives like the circular economy package of the EU. Purely from a recycling point of view, this study shows that FBC-IBA has some major advantages over GI-IBA. Metals recovered from FBC-IBA are qualitatively more suitable for recycling as they are generally less oxidized than metals from the GI-IBA. These metals are concentrated in larger particle-size-fractions, making a recovery significantly easier. This finding is important from an economic and environmental point of view since metals have a significant monetary value and the primary production of metals causes more environmental burden than recycling. A high recovery rate of metals also facilitates the utilization of glass and mineral materials, as both routes require low metal contents. Since almost 50 % of the FBC-IBA consists of glass, from which three-quarters have a particle size >8 mm, and in addition, this glass fraction is less contaminated compared to the GI-IBA, it is worth investigating the quality and recovery methods of this material in more detail. For utilization in the construction sector, minerals from the FBC-IBA also show more promising results due to the lower total content of heavy metals and their preferable leaching behavior. In-depth mineralogical investigations, such as X-ray diffraction (XRD), differential thermal analysis (DTA) and thermogravimetric analysis (TGA), can help to further understand and explain the differences between the two IBAs.

From a quantitative point of view, more aluminum and significantly more glass can be recovered from the FBC-IBA based on the plant input. For other metals, the incineration technology has no significant influence on the recovery potential.

Many of the discussed advantages of the FBC-IBA are due to a combination of a more homogeneous input (e.g., pretreatment of the waste), the conditions in the incinerator (e.g., lower bed temperature, more homogeneous temperature distribution), and the dry IBA

discharge.

However, it is not possible to assess which incineration technology is better in terms of a circular economy and from an environmental point of view purely on the basis of a comparison of the IBAs. For this purpose, the entire incineration processes, including their pre-processes (e.g., pretreatment of MSW), the energy recoverable from waste and the possible applications for IBA utilization, must be considered. An overall assessment must also consider that fines are transferred to fly ash (IFA) in an FBC. This results in about five times more IFA per unit of waste incinerated compared to a GI, which has to be landfilled. However, this can also be desirable, as the fine fraction contains more pollutants, and concentrating them in IFA, removes them from the materials cycle.

Declaration of Competing Interest

The authors declare that they have no known competing financial interests or personal relationships that could have appeared to influence the work reported in this paper.

Data availability

The authors do not have permission to share data.

Acknowledgments

The work presented is part of two large-scale research initiatives on anthropogenic resources (Christian Doppler Laboratory for Anthropogenic Resources) and circular economy (Christian Doppler Laboratory for a Recycling-based Circular Economy). The financial support by the Austrian Federal Ministry for Digital and Economic Affairs, the National Foundation for Research, Technology and Development and the Christian Doppler Research Association is gratefully acknowledged. Industry partners co-financing this study were Wien Energie GmbH and Wiener Kommunal-Umweltschutzprojektgesellschaft GmbH (WKU). The authors express their gratitude to the municipal department 48 of the City of Vienna for its essential contribution to the experiments. The support of Philipp Aschenbrenner, Jost Gadermaier, Manuel Hahn, Helene Lutz, Zsombor Major, Ole Mallow and Klaus Stücklschwaiger with sampling, sample preparation and chemical analysis is gratefully acknowledged. The authors also acknowledge TU Wien University Library for financial support through its Open Access Funding Program, and the assistance given by the City of Vienna.

Appendix A. Supplementary material

Supplementary data to this article can be found online at https://doi.org/10.1016/j.wasman.2023.02.021.

References

Abbà, A., Collivignarelli, M.C., Sorlini, S., Bruggi, M., 2014. On the reliability of reusing bottom ash from municipal solid waste incineration as aggregate in concrete. Compos. Part B: Eng. 58, 502–509. https://doi.org/10.1016/j.compositesb.2013.11.008.

Abbas, Z., Steenari, B.-M., Lindqvist, O., 2001. A study of Cr(VI) in ashes from fluidized bed combustion of municipal solid waste: leaching, secondary reactions and the applicability of some speciation methods. Waste Manag. 21, 725–739. https://doi.org/10.1016/S0956-053X(01)00005-8.

Abdullah, M.H., Rashid, A.S.A., Anuar, U.H.M., Marto, A., Abuelgasim, R., 2019. Bottom ash utilization: A review on engineering applications and environmental aspects. IOP Conf. Series: Mater. Sci. Eng. 527, 012006 https://doi.org/10.1088/1757-899x/527/1/012006.

Alam, Q., Schollbach, K., van Hoek, C., van der Laan, S., de Wolf, T., Brouwers, H.J.H., 2019. In-depth mineralogical quantification of MSWI bottom ash phases and their association with potentially toxic elements. Waste Manag. 87, 1–12. https://doi.org/10.1016/j.wasman.2019.01.031.

Astrup, T., Muntoni, A., Polettini, A., Pomi, R., Van Gerven, T., Van Zomeren, A., 2016. Chapter 24 - treatment and reuse of incineration bottom ash. In: Prasad, M.N.V., Shih, K. (Eds.), Environmental Materials and Waste. Academic Press, pp. 607–645. https://doi.org/10.1016/B978-0-12-803837-6.00024-X.

Blasenbauer, D., Huber, F., Lederer, J., Quina, M.J., Blanc-Biscarat, D., Bogush, A., Bontempi, E., Blondeau, J., Chimenos, J.M., Dahlbo, H., Fagerqvist, J., Giro-Paloma, J., Hjelmar, O., Hyks, J., Keaney, J., Lupsea-Toader, M., O'Caollai, C.J., Orupõld, K., Pająk, T., Simon, F.-G., Svecova, L., Šyc, M., Ulvang, R., Vaajasaari, K., Van Caneghem, J., van Zomeren, A., Vasarevičius, S., Wégner, K., Fellner, J., 2020. Legal situation and current practice of waste incineration bottom ash utilisation in Europe. Waste Manag. 102, 868–883. https://doi.org/10.1016/j.wasman.2019.11.031.

Boehmer, S., Kübler, I., Stoiber, H., Walter, B., 2006. Abfallverbrennung in Österreich Statusbericht 2006 (Waste incineration in Austria Status Report 2006). Umweltbundesamt Österreich (Environment Agency Austria), Austria, https://www.data.gv.at/katalog/en/dataset/abfallverbrennunginsterreich.

Brunner, P.H., Mönch, H., 1988. The flux of metals through municipal solid waste incinerators**ISWA specialized seminar incinerator emissions of heavy metals and particulates. In: Dean, R.B. (Ed.), Incineration of Municipal Waste. Academic Press, pp. 103–117. https://doi.org/10.1016/B978-0-12-207690-9.50014-3.

Bruno, M., Abis, M., Kuchta, K., Simon, F.G., Gronholm, R., Hoppe, M., Fiore, S., 2021. Material flow, economic and environmental assessment of municipal solid waste incineration bottom ash recycling potential in Europe. J. Clean. Prod. 317, 13. https://doi.org/10.1016/j.jclepro.2021.128511.

Bunge, R., 2018. Recovery of metals from waste incineration bottom ash. In: Holm, O., Thome-Kozmiensky, E. (Eds.), Removal, Treatment and Utilisation of Waste Incineration Bottom Ash. TK Verlag, Neuruppin Germany, pp. 63–143.

Caviglia, C., Confalonieri, G., Corazzari, I., Destefanis, E., Mandrone, G., Pastero, L., Boero, R., Pavese, A., 2019. Effects of particle size on properties and thermal inertization of bottom ashes (MSW of Turin's incinerator). Waste Manag. 84, 340–354. https://doi.org/10.1016/j.wasman.2018.11.050.

Chandler, A.J., Eighmy, T.T., Hartlen, J., Hjelmar, O., Kosson, D.S., Sawell, S.E., van der Sloot, H.A., Vehlow, J., 1997. Municipal solid waste incinerator residues: An international perspective on characterisation and management of residues from municipal solid waste incineration. Elsevier Science, Amsterdam.

Chimenos, J.M., Segarra, M., Fernández, M.A., Espiell, F., 1999. Characterization of the bottom ash in municipal solid waste incinerator. J. Hazard. Mater. 64, 211–222. https://doi.org/10.1016/S0304-3894(98)00246-5.

Cornelis, G., Van Gerven, T., Vandecasteele, C., 2006. Antimony leaching from uncarbonated and carbonated MSWI bottom ash. J. Hazard. Mater. 137, 1284–1292. https://doi.org/10.1016/j.jhazmat.2006.04.048.

Cornelis, G., Gerven, T.V., Vandecasteele, C., 2012. Antimony leaching from MSWI bottom ash: Modelling of the effect of pH and carbonation. Waste Manag. 32, 278–286. https://doi.org/10.1016/j.wasman.2011.09.018.

De Gisi, S., Chiarelli, A., Tagliente, L., Notarnicola, M., 2018. Energy, environmental and operation aspects of a SRF-fired fluidized bed waste-to-energy plant. Waste Manag. 73, 271–286. https://doi.org/10.1016/j.wasman.2017.04.044.

del Valle-Zermeño, R., Gómez-Manrique, J., Giro-Paloma, J., Formosa, J., Chimenos, J. M., 2017. Material characterization of the MSWI bottom ash as a function of particle size. Effects of glass recycling over time. Sci. Total Environ. 581–582, 897–905. https://doi.org/10.1016/j.scitotenv.2017.01.047.

Dou, X., Ren, F., Nguyen, M.Q., Ahamed, A., Yin, K., Chan, W.P., Chang, V.-W.-C., 2017. Review of MSWI bottom ash utilization from perspectives of collective characterization, treatment and existing application. Renew. Sustain. Energy Rev. 79, 24–38. https://doi.org/10.1016/j.rser.2017.05.044.

Dugenest, S., Combrisson, J., Casabianca, H., Grenier-Loustalot, M.F., 1999. Municipal solid waste incineration bottom ash: Characterization and kinetic studies of organic matter. Environ. Sci. Tech. 33, 1110–1115. https://doi.org/10.1021/es980193e.

EN, 2002. EN 12457-4:2002 - Characterisation of waste - Leaching - Compliance test for leaching of granular waste materials and sludges - Part 4: One stage batch test at a liquid to solid ratio of 10 l/kg for materials with particle size below 10 mm (without or with size reduction).

Fellner, J., Lederer, J., Purgar, A., Winterstetter, A., Rechberger, H., Winter, F., Laner, D., 2015. Evaluation of resource recovery from waste incineration residues – The case of zinc. Waste Manag. 37, 95–103. https://doi.org/10.1016/j.wasman.2014.10.010.

Hjelmar, O., Van der Sloot, H., Van Zomeren, A., 2013. Hazard Properties Classification of High Temperature Waste Materials, Sardinia 2013, Fourteenth International Waste Management and Landfill Symposium, 30 September – 4 October 2013. CISA Publisher, Italy, Sardinia, Italy.

Holm, O., Simon, F.-G., 2017. Innovative treatment trains of bottom ash (BA) from municipal solid waste incineration (MSWI) in Germany. Waste Manag. 59, 229–236. https://doi.org/10.1016/j.wasman.2016.09.004.

Hu, Y., Bakker, M.C.M., de Heij, P.G., 2011. Recovery and distribution of incinerated aluminum packaging waste. Waste Manag. 31, 2422–2430. https://doi.org/10.1016/j.wasman.2011.07.021.

Huber, F., 2020. Modelling of material recovery from waste incineration bottom ash. Waste Manag. 105, 61–72. https://doi.org/10.1016/j.wasman.2020.01.034.

Huber, F., Blasenbauer, D., Aschenbrenner, P., Fellner, J., 2019. Chemical composition and leachability of differently sized material fractions of municipal solid waste incineration bottom ash. Waste Manag. 95, 593–603. https://doi.org/10.1016/j.wasman.2019.06.047.

Huber, F., Blasenbauer, D., Aschenbrenner, P., Fellner, J., 2020. Complete determination of the material composition of municipal solid waste incineration bottom ash. Waste Manag. 102, 677–685. https://doi.org/10.1016/j.wasman.2019.11.036.

Huber, F., Korotenko, E., Šyc, M., Fellner, J., 2021. Material and chemical composition of municipal solid waste incineration bottom ash fractions with different densities. J. Mater. Cycles Waste Manage. 23, 394–401. https://doi.org/10.1007/s10163-020-01109-z.

Johnson, C.A., Kaeppeli, M., Brandenberger, S., Ulrich, A., Baumann, W., 1999. Hydrological and geochemical factors affecting leachate composition in municipal

solid waste incinerator bottom ash: Part II. The geochemistry of leachate from Landfill Lostorf, Switzerland. J. Contam. Hydrol. 40, 239–259. https://doi.org/10.1016/S0169-7722(99)00052-2.
Jung, C.H., Matsuto, T., Tanaka, N., Okada, T., 2004. Metal distribution in incineration residues of municipal solid waste (MSW) in Japan. Waste Manag. 24, 381–391. https://doi.org/10.1016/S0956-053X(03)00137-5.
Kalbe, U., Simon, F.-G., 2020. Potential use of incineration bottom ash in construction: Evaluation of the environmental impact. Waste Biomass Valoriz. 11, 7055–7065. https://doi.org/10.1007/s12649-020-01086-2.
Kirnbauer, F., Kraft, S., 2017. Energy Recovery from High Calorific Fractions by Incineration together with Sewage Sludge in the Fluidized Bed Furnace in Simmeringer Haide, In: Thomé-Kozmiensky, K.J., Thiel, S., Thomé-Kozmiensky, E., Winter, F., Juchelková, D. (Eds.), Waste Management, Volume 7 – Waste-to-Energy –. TK Verlag, Neuruppin Germany, 315–328.
Kolbitsch, P., Madl, F., Wachter, R., 2012. Construction and Operating Experiences of the RHKW Linz (Austria). TK Verlag, pp. 317–326.
Krobath, P., Thomé-Kozmiensky, K.J., 2004. The new fluidized bed furnace for the incineration of sewage sludge and refuse derived fuel (Original title: Der neue Wirbelschichtofen zur Verbrennung von Klärschlamm und Ersatzbrennstoff). In: Kossina, I. (Ed.), Waste Management for Vienna (Original title: Abfallwirtschaft für Wien). TK Verlag Karl Thomé-Kozmiensky, Neuruppin, Germany, pp. 197–238.
Leckner, B., Lind, F., 2020. Combustion of municipal solid waste in fluidized bed or on grate – A comparison. Waste Manag. 109, 94–108. https://doi.org/10.1016/j.wasman.2020.04.050.
Loginova, E., Volkov, D.S., van de Wouw, P.M.F., Florea, M.V.A., Brouwers, H.J.H., 2019. Detailed characterization of particle size fractions of municipal solid waste incineration bottom ash. J. Clean. Prod. 207, 866–874. https://doi.org/10.1016/j.jclepro.2018.10.022.
Luo, H., Cheng, Y., He, D., Yang, E.-H., 2019. Review of leaching behavior of municipal solid waste incineration (MSWI) ash. Sci. Total Environ. 668, 90–103. https://doi.org/10.1016/j.scitotenv.2019.03.004.
Maldonado-Alameda, A., Mañosa, J., Miro-Escola, J., Quintero-Payan, A.C., Chimenos, J.M., 2023. Fluidised-bed incineration bottom ash as the sole precursor of alkali-activated binders: A comparison with bottom ash from grate incinerators. Constr. Build. Mater. 364, 130001 https://doi.org/10.1016/j.conbuildmat.2022.130001.
Morf, L.S., Gloor, R., Haag, O., Haupt, M., Skutan, S., Lorenzo, F.D., Böni, D., 2013. Precious metals and rare earth elements in municipal solid waste – Sources and fate in a Swiss incineration plant. Waste Manag. 33, 634–644. https://doi.org/10.1016/j.wasman.2012.09.010.
Muchova, L., Bakker, E., Rem, P., 2009. Precious Metals in Municipal Solid Waste Incineration Bottom Ash. Water Air Soil Pollut. Focus 9, 107–116. https://doi.org/10.1007/s11267-008-9191-9.
Mühl, J., Feher, F., Skutan, S., Stockinger, G., Lederer, J., 2022. Rost- oder Wirbelschichtfeuerung bei Abfallverbrennungsanlagen: Was ist aus Sicht der Kreislaufwirtschaft von MVA-Aschen zu bevorzugen? (Grate Furnace or Fluidized Bed in Municipal Solid Waste Incineration Plants: What to Prefer from the View of a Circular Economy of MSWI-Ashes?), In: Thiel, S., Thomé-Kozmiensky, E., Senk, D.G., Wotruba, H., Antrekowitsch, H., Pomberger, R. (Eds.), Mineralische Nebenprodukte und Abfälle, Band 9, 228–245.
Pomberger, R., Sarc, R., Lorber, K.E., 2017. Dynamic visualisation of municipal waste management performance in the EU using ternary diagram method. Waste Manag. 61, 558–571. https://doi.org/10.1016/j.wasman.2017.01.018.
Purgar, A., Winter, F., Blasenbauer, D., Hartmann, S., Fellner, J., Lederer, J., Rechberger, H., 2016. Main drivers for integrating zinc recovery from fly ashes into the Viennese waste incineration cluster. Fuel Process. Technol. 141, 243–248. https://doi.org/10.1016/j.fuproc.2015.10.003.
Republic of Austria, 2017a. Bundesabfallwirtschaftsplan 2017 - Teil 1 (Federal Waste Management Plan 2017). Bundesministerium für Nachhaltigkeit und Tourismus.
Republic of Austria, 2017b. Technische Grundlagen für den Einsatz von Abfällen als Ersatzrohstoffe in Anlagen zur Zementerzeugung (English: Technical basics for the use of waste as secondary raw material in cement production.). Federal Ministry of Agriculture, Forestry, Environment and Water Management, Austria.
Riber, C., Bhander, G.S., Christensen, T.H., 2008. Environmental assessment of waste incineration in a life-cycle-perspective (EASEWASTE). Waste Manag. Res. 26, 96–103. https://doi.org/10.1177/0734242X08088583.
Saikia, N., Cornelis, G., Mertens, G., Elsen, J., Van Balen, K., Van Gerven, T., Vandecasteele, C., 2008. Assessment of Pb-slag, MSWI bottom ash and boiler and fly ash for using as a fine aggregate in cement mortar. J. Hazard. Mater. 154, 766–777. https://doi.org/10.1016/j.jhazmat.2007.10.093.
Santos, R.M., Mertens, G., Salman, M., Cizer, Ö., Van Gerven, T., 2013. Comparative study of ageing, heat treatment and accelerated carbonation for stabilization of municipal solid waste incineration bottom ash in view of reducing regulated heavy metal/metalloid leaching. J. Environ. Manage. 128, 807–821. https://doi.org/10.1016/j.jenvman.2013.06.033.
Scarlat, N., Fahl, F., Dallemand, J.-F., 2019. Status and opportunities for energy recovery from municipal solid waste in Europe. Waste Biomass Valoriz. 10, 2425–2444. https://doi.org/10.1007/s12649-018-0297-7.
Seniunaite, J., Vasarevicius, S., 2017. Leaching of copper, lead and zinc from municipal solid waste incineration bottom ash. Energy Procedia 113, 442–449. https://doi.org/10.1016/j.egypro.2017.04.036.
Simon, F.G., Vogel, C., Kalbe, U., 2021. Antimony and vanadium in incineration bottom ash – leaching behavior and conclusions for treatment processes. Detritus 16, 75–81. https://doi.org/10.31025/2611-4135/2021.15115.
Šyc, M., Krausová, A., Kameníková, P., Šomplák, R., Pavlas, M., Zach, B., Pohořelý, M., Svoboda, K., Punčochář, M., 2018. Material analysis of Bottom ash from waste-to-energy plants. Waste Manag. 73, 360–366. https://doi.org/10.1016/j.wasman.2017.10.045.
Šyc, M., Simon, F.G., Hykš, J., Braga, R., Biganzoli, L., Costa, G., Funari, V., Grosso, M., 2020. Metal recovery from incineration bottom ash: State-of-the-art and recent developments. J. Hazard. Mater. 393, 122433 https://doi.org/10.1016/j.jhazmat.2020.122433.
Turner, A., Filella, M., 2020. Antimony in paints and enamels of everyday items. Sci. Total Environ. 713, 136588 https://doi.org/10.1016/j.scitotenv.2020.136588.
Van Caneghem, J., Van Acker, K., De Greef, J., Wauters, G., Vandecasteele, C., 2019. Waste-to-energy is compatible and complementary with recycling in the circular economy. Clean Technol. Environ. Policy 21, 925–939. https://doi.org/10.1007/s10098-019-01686-0.
Vandecasteele, C., Wauters, G., Arickx, S., Jaspers, M., Van Gerven, T., 2007. Integrated municipal solid waste treatment using a grate furnace incinerator: The Indaver case. Waste Manag. 27, 1366–1375. https://doi.org/10.1016/j.wasman.2006.08.005.
Vateva, I., Laner, D., 2020. Grain-size specific characterisation and resource potentials of municipal solid waste incineration (MSWI) bottom ash: A german case study. Resources 9. https://doi.org/10.3390/resources9060066.
Verbinnen, B., Billen, P., Van Caneghem, J., Vandecasteele, C., 2017. Recycling of MSWI bottom ash: A review of chemical barriers, engineering applications and treatment technologies. Waste Biomass Valoriz. 8, 1453–1466. https://doi.org/10.1007/s12649-016-9704-0.
Viczek, S.A., Aldrian, A., Pomberger, R., Sarc, R., 2020. Origins and carriers of Sb, As, Cd, Cl, Cr Co, Pb, Hg, and Ni in mixed solid waste – A literature-based evaluation. Waste Manag. 103, 87–112. https://doi.org/10.1016/j.wasman.2019.12.009.
Wei, Y., Shimaoka, T., Saffarzadeh, A., Takahashi, F., 2011. Mineralogical characterization of municipal solid waste incineration bottom ash with an emphasis on heavy metal-bearing phases. J. Hazard. Mater. 187, 534–543. https://doi.org/10.1016/j.jhazmat.2011.01.070.
Wissing, F., Wirtz, S., Scherer, V., 2017. Simulating municipal solid waste incineration with a DEM/CFD method – Influences of waste properties, grate and furnace design. Fuel 206, 638–656. https://doi.org/10.1016/j.fuel.2017.06.037.